Dalton Transactions

PAPER

View Article Online
View Journal | View Issue

Open Access Article. Published on 05 February 2015. Downloaded on 12/4/2025 9:05:27 PM.
This article is licensed under a Creative Commons Attribution 3.0 Unported Licence.

Cite this: *Dalton Trans.*, 2015, **44**, 5153

Received 14th January 2015,
Accepted 5th February 2015

DOI: 10.1039/c5dt00172b

www.rsc.org/dalton

Te–Te and Te–C bond cleavage reactions using a monovalent gallanediyl†

Chelladurai Ganesamoorthy, Georg Bendt, Dieter Bläser, Christoph Wölper and Stephan Schulz*

LGa (L = [(2,6-i-Pr_2-C_6H_3)NC(Me)]$_2$CH) reacts with elemental tellurium with formation of the Te-bridged compound [LGa-μ-Te]$_2$ **1**, whereas the reactions with Ph_2Te_2 and i-Pr_2Te occurred with cleavage of the Te–Te and Te–C bond, respectively, and subsequent formation of LGa(TePh)$_2$ **2** and LGa(i-Pr)Tei-Pr **3**. **1–3** were characterized by heteronuclear NMR (^{1}H, ^{13}C, ^{125}Te) and IR spectroscopy and their solid state structures were determined by single crystal X-ray analyses.

Introduction

Univalent LGa containing the sterically crowded β-diketiminate ligand (L = [(2,6-i-Pr_2-C_6H_3)NC(Me)]$_2$CH)[1] adopts a monomeric structure in the solid state and in solution. The gallium valence shell contains two bond pairs, a lone pair and an empty p-orbital. Therefore, LGa can react as electrophilic and nucleophilic reagent at the gallium atom. Computational calculations predicted that LGa is a good σ-donor but a poor π-acceptor due to the low energy and high s-character of the HOMO, and the large energy difference (95.3–110 kcal mol^{-1}) between the HOMO and the rather diffuse acceptor 4p-orbital (LUMO+1).[2–4] The σ-donor capacity of LGa was experimentally demonstrated for instance with the synthesis of the Lewis acid–base adduct LGa→B(C_6F_5)$_3$ [5] and other p- or d-block metal complexes as well as with the synthesis of a large variety of (late) transition metal complexes.[6] The latter were shown to be promising reagents for the activation of small molecules such as ethylene and have been used as precursors for the formation of heterometallic clusters,[7,8] which in part can be described as molecular models for alloys.

While the coordination chemistry of LGa has been developed to a far greater extent compared to that of its lighter homologue LAl, its use in the transformation of unsaturated organic substrates has not,[9–11] which most likely results from the weaker reducing properties of LGa. However, LGa was found to react with E–X bonds *via* insertion of the Ga(I) centre and subsequent formation of covalent Ga–E bonds.[12] This reaction pathway was used for cluster formation reactions *via* oxidative insertion/reductive elimination processes. The synthesis of molecular gallium–tin intermetallic clusters upon reaction of LGa with $SnCl_2$ [13] as well as two galla-dibismuthenes containing covalent Ga–Bi single-bonds and Bi=Bi double bonds, which were obtained from the reactions of LGa with Bi(OR)$_3$ (R = O_2SCF_3, C_6F_5),[14] represent remarkable experimental "snapshots" of these reactions. The cluster compounds can be considered as isolated reaction intermediates on the way to full reduction to tin metal and bismuth metal, respectively. The syntheses of these complexes demonstrate the promising potential of LGa to serve as selective reducing agent in the preparation of metalloid clusters and subvalent "metastable" compounds.

In addition to these interesting studies on the synthesis of intermetallic compounds, the capability of LGa in bond activation reactions was also studied. LGa was reacted with a large variety of compounds containing different element–element bonds including dihydrogen[15] as well as electronically unsaturated molecules such as N_2O, organic azides N_3R and elemental sulphur. Many of these reactions were performed in order to synthesize compounds containing multiple bonds to gallium. However, reactions of LGa with N_2O or S_8 yielded the oxo- or sulfido bridged dimers [LGa-μ-E]$_2$ (E = O, S),[16] while its reaction with N_3SiMe_3 proceeded with formation of a cyclic gallium tetrazole and a gallium imide/azide compound. The most-likely formed reaction intermediate, a monomeric gallium imide LGa=NR,[17] was finally synthesized by reaction of LGa with the sterically encumbered azide Ar*N_3 (Ar* = 2,6-Trip$_2$-C_6H_3, Trip = 2,4,6-i-Pr_3-C_6H_2) and structurally characterized by single crystal X-ray diffraction.[18]

Our long-term interest in the reactivity of low-valent organometallics of group 12 to 16 elements prompted us to start investigations on the general reactivity of LM (M = Al, Ga, In)

Institute of Inorganic Chemistry, University of Duisburg-Essen, 45117 Essen, Germany. E-mail: stephan.schulz@uni-due.de; Fax: +201 1833830; Tel: +201 1834635

† Electronic supplementary information (ESI) available: Crystallographic data of **1a**, **1b**, **2**, and **3** and spectroscopic details (^{1}H, ^{13}C, ^{125}Te, IR). CCDC 1040132–1040135. For ESI and crystallographic data in CIF or other electronic format see DOI: 10.1039/c5dt00172b

Open Access Article. Published on 05 February 2015. Downloaded on 12/4/2025 9:05:27 PM.
This article is licensed under a Creative Commons Attribution 3.0 Unported Licence.

toward group 15 compounds such as $BiEt_3$ [19] as well as tetraalkyldistibanes and dibismuthanes Et_4E_2 (E = Sb, Bi).[20] These reactions were found to proceed with cleavage of the Bi–C as well as E–E bond and subsequent formation of $LM(Et)BiEt_2$ and $LM(EEt_2)_2$, respectively, in which the Ga atom is oxidized from the formal oxidation state +I to +III. Moreover, oxidative addition reactions of monovalent Zn(I) compounds,[21] germylenes and stannylenes[22] as well as distibanes and dibismuthanes[23] with dichalcogenanes were reported by us. In addition, insertion reactions of elemental chalcogens into metal–metal bonds were observed in reactions with tetraalkyldistibanes and -dibismuthanes.[24,25] We herein report on the reactions of LGa with elemental tellurium as well as diphenylditellane Ph_2Te_2 and diisopropyltellane i-Pr_2Te, which proceeded with Te–Te and Te–C bond cleavage and subsequent formation of compounds containing direct Ga–Te σ-bonds.

Results and discussion

Equimolar amounts of LGa were reacted with elemental tellurium, diphenylditellane Ph_2Te_2 and diisopropyltellane i-Pr_2Te in toluene at ambient temperature, yielding the Te-bridged dimer $[LGa\text{-}\mu\text{-}Te]_2$ **1** as well as $LGa(TePh)_2$ **2** and LGa(i-Pr)Tei-Pr **3**, respectively (Scheme 1). **1–3** are moisture sensitive, yellow to pale yellow crystalline solids but moderately stable toward air. **1** is sparingly soluble in benzene, toluene and *n*-hexane whereas **2** and **3** are soluble in these solvents.

The ^1H and ^{13}C NMR spectra of **1–3** show the characteristic resonances of the organic entities. ^1H NMR spectral pattern of **1** and **2** are similar to those of LGa and C_{2v} symmetric molecules related to the β-diketiminate ligands. They exhibit single resonances for the γ-CH (4.59 ppm, **1**; 4.76 ppm, **2**) and two methyl groups of the C_3N_2Ga rings (1.35 ppm **1**; 1.50 ppm **2**). The methyl protons of the isopropyl substituents and methine protons appear as two doublets (1.13 & 1.10 ppm **1**; 1.48 & 1.08 ppm **2**) and a septet (3.33 ppm **1**; 3.62 ppm **2**), respectively. Due to its low solubility, the ^{13}C and ^{125}Te NMR resonances of **1** were not intense enough. The ^{13}C NMR spectrum of **2** shows 14 signals including the characteristic resonances due to the γ-CH (99.22 ppm) backbone carbon atom, both β-C atoms atoms of the C_3N_2Ga ring (170.63 ppm) and the methine (29.36 ppm) and methyl carbon atoms of isopropyl groups (27.01, 25.44 ppm). Compound **3** shows more distinct ^1H and ^{13}C NMR patterns than **1** and **2**. Due to the presence of three different substituents at the Ga atom and a hindered rotation about the N–C bonds, the i-Pr groups in **3** are magnetically inequivalent, leading to six doublets (1.87, 1.61, 1.34, 1.31, 1.08, 0.67 ppm) in the ^1H NMR spectrum. The six methine protons of the i-Pr groups appear as four septets (4.16, 3.82, 3.42, 1.04 ppm) with the integral ratios of 2 : 1 : 2 : 1, respectively. Integrals of 2 H belong to the i-Pr methine groups of the L ligand. The γ-CH and two methyl groups of the C_3N_2M ring are in the mirror plane and exhibit only single resonances at 4.67 and 1.51 ppm, respectively. The $^{13}C\{^1H\}$ NMR spectrum of **3** shows the expected 19 signals and some of them were tentatively assigned to the i-Pr carbons atoms in **3** in the Experimental section. Elemental analyses (C, H, N) of **1–3** confirm the structural compositions and their analytical pure nature. Furthermore, the NMR (^1H, ^{13}C, ^{125}Te) and IR spectroscopic details are in accordance with the proposed formulations of **1–3**.

1–3 are stable in solution and no reduction/decomposition occurs even at 90 °C in C_6D_6. Despite that the first Te–C bond cleavage of i-Pr_2Te occurred smoothly at room temperature, the second Te–C bond couldn't be cleaved by reaction with an additional equivalent of LGa. In contrast, we successfully cleaved the Te–C and Te–Te bonds of Ph_2Te_2 upon reaction with an equimolar amount of the Lewis acid–base adduct $LGa{\rightarrow}B(C_6F_5)_3$ in C_6D_6, which yielded an yellow-orange solution at room temperature within three days. The ^1H NMR spectrum of the reaction mixture shows the presence of four different types of γ-CH protons with different integral ratios (Fig. S11†) and the spectral comparison evidences the presence of traces of **1** (4.57, 3.39 ppm) and **2** (4.76, 3.62 ppm) along with two unknown compounds. Prolonged storage of the reaction mixture (10 days) at room temperature led to pale yellow crystals of **1**. During this period the peaks corresponding to **2** gradually decreased. Unfortunately, our efforts to isolate the major component of the reaction mixture (see Fig. S12†) failed since the solution is highly sensitive and decomposes to oily substances. According to the ^1H NMR pattern, the Ga atom in the major product has three different substituents.

Single crystals of **1** were grown separately in benzene and toluene solutions. **1a** is the solvent-free compound (obtained from the 1 : 1 reaction of Ph_2Te_2 and $LGa{\rightarrow}B(C_6F_5)_3$) and crystallises in the monoclinic space group $P2_1/n$, while **1b** is its toluene hemi-solvate (obtained from the 1 : 1 reaction of Te and LGa), which crystallises in the monoclinic space group $C2/m$. Single crystals of **2** were obtained from a freshly prepared *n*-hexane solution upon storage at room temperature,

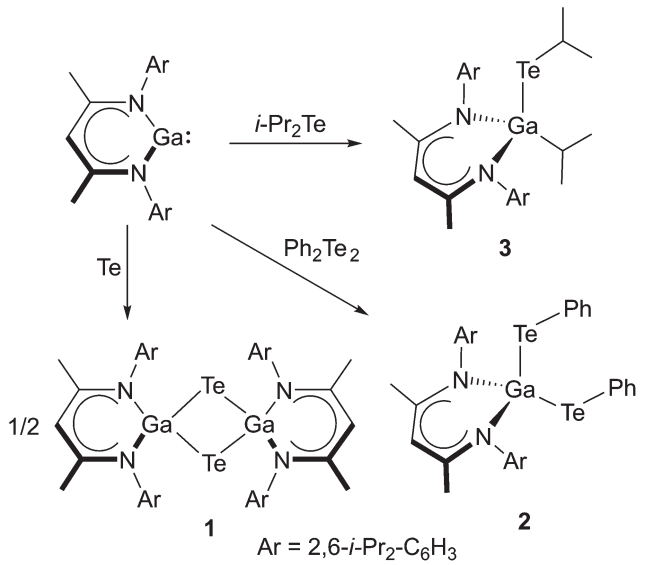

Scheme 1 Synthesis of **1–3**.

Open Access Article. Published on 05 February 2015. Downloaded on 12/4/2025 9:05:27 PM.
This article is licensed under a Creative Commons Attribution 3.0 Unported Licence.

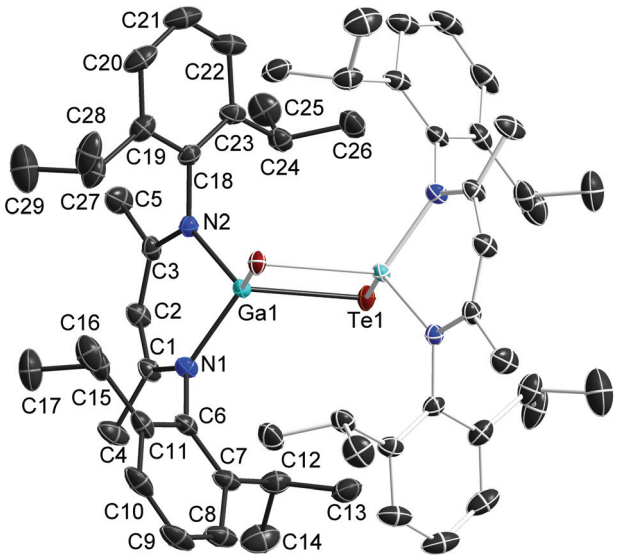

Fig. 1 Solid state structure of **1a** (thermal ellipsoids are shown at 50% probability levels); H atoms are omitted for clarity. Symmetry generated part in pale colours. Selected bond lengths and angles in Å and °: Te(1)–Ga(1)#1 2.5777(4), Te(1)–Ga(1) 2.5898(4), Ga(1)–N(2) 1.979(2), Ga(1)–N(1) 1.982(2), C(1)–C(2) 1.397(4), C(2)–C(3) 1.397(4), N(1)–C(1) 1.339(4), N(2)–C(3) 1.337(4), N(2)–Ga(1)–N(1) 94.92(10), N(2)–Ga(1)–Te(1)#1 118.56(7), N(1)–Ga(1)–Te(1)#1 115.72(7), N(2)–Ga(1)–Te(1) 114.87(7), N(1)–Ga(1)–Te(1) 115.13(7), Te(1)#1–Ga(1)–Te(1) 98.883(11), C(3)–C(2)–C(1) 128.4(3), N(1)–C(1)–C(2) 123.6(3), N(2)–C(3)–C(2) 124.1(3).

while single crystals of **3** were grown from saturated toluene solutions at 5 °C. **2** and **3** crystallise in the orthorhombic space groups *Pbca* (**2**) and *Pnma* (**3**). Fig. 1–3 show the solid state structures of **1a**, **2** and **3** and the selected bond lengths and bond angles are given at the figure captions. Table 1 summarizes the crystal data and details of the structural determinations.

The Ga atoms in **1a**, **1b**, **2** and **3** each adopt slightly distorted tetrahedral coordination spheres.‡ The six-membered GaN_2C_3 rings show *boat-type* conformations, in which the Ga atoms are significantly out of-plane (deviation from best plane of the ligand's backbone: 0.521(3) Å **1a**, 0.5853(19) and 0.560(2) Å **1b**, 0.721(5) Å **2**, 0.6309(18) Å **3**) The average Ga–N bond length (1.981(2) Å **1a**; 1.992(2) Å **1b**; 1.961(4) Å **2**; 1.9739(10) Å **3**) and N–Ga–N bond angle (94.92(10)° **1a**; 95.38(6)° **1b**; 97.45(15)° **2**; 95.66(5)° **3**) as observed for **1**, **2** and **3** are almost identical to that of LGa, for which an average Ga–N distance of 2.054(2) Å and a N–Ga–N bond angle of 87.56(6)° was reported.[1] The Te–Ga–Te (98.88(2)° **1a**; 100.39(1)° **1b**; 113.59(2)° **2**) and C–Ga–Te bond angles (105.84(5)° **3**) are smaller compared to the N–Ga–N bond angles. The Ga–Te bond lengths (2.5777(4), 2.5898(4) Å **1a**; 2.5809(2), 2.5909(2) Å **1b**; 2.5586(5), 2.6076(6) Å **2**; 2.5929(4) Å **3**) are comparable to those reported for $[K(OEt_2)_3][(PhTe)_2Ga\{[N(2,6\text{-i-}Pr_2\text{-}C_6H_3)\text{-}C(H)]_2\}]$ (2.5785(12), 2.6577(10) Å),[26] the Te-bridged dimers

‡The crystallographic data of **1a**, **1b**, **2**, and **3** (excluding structure factors) have been deposited with the Cambridge Crystallographic Data Centre as supplementary publication nos. CCDC-1040132 (**1a**), CCDC-1040134 (**1b**), CCDC-1040133 (**2**) and CCDC-1040135 (**3**).

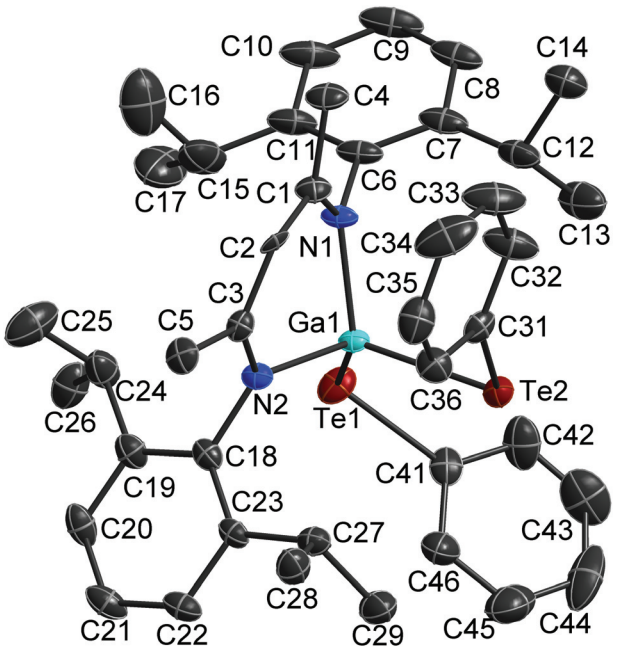

Fig. 2 Solid state structure of **2** (thermal ellipsoids are shown at 50% probability levels); H atoms are omitted for clarity. Selected bond lengths and angles in Å and °: Ga(1)–N(1) 1.950(4), Ga(1)–N(2) 1.971(4), Ga(1)–Te(1) 2.5586(5), Ga(1)–Te(2) 2.6076(6), Te(1)–C(41) 2.114(5), Te(2)–C(31) 2.144(4), N(1)–C(1) 1.342(6), N(2)–C(3) 1.334(5), C(1)–C(2) 1.377(6), C(2)–C(3) 1.406(6), N(1)–Ga(1)–N(2) 97.45(15), N(1)–Ga(1)–Te(1) 110.65(11), N(2)–Ga(1)–Te(1) 114.06(11), N(1)–Ga(1)–Te(2) 110.98(12), N(2)–Ga(1)–Te(2) 109.00(11), Te(1)–Ga(1)–Te(2) 113.587(19), C(1)–C(2)–C(3) 130.5(4), N(1)–C(1)–C(2) 123.5(4), N(2)–C(3)–C(2) 122.7(4).

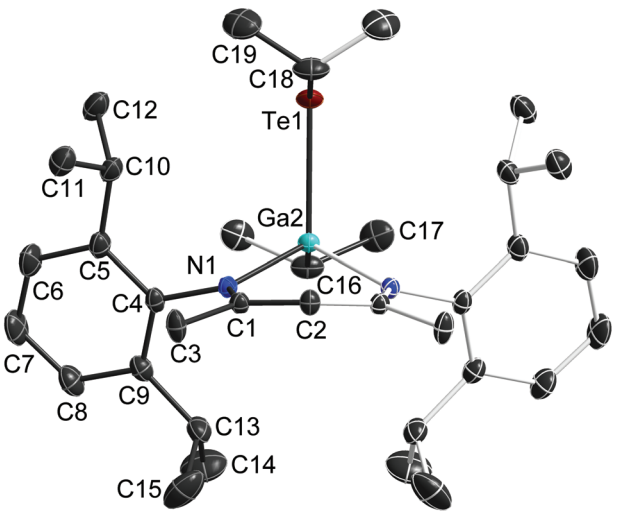

Fig. 3 Solid state structure of **3** (thermal ellipsoids are shown at 50% probability levels); H atoms are omitted for clarity. Symmetry generated part in pale colours. Selected bond lengths and angles in Å and °: Te(1)–C(18) 2.1983(19), Te(1)–Ga(2) 2.5929(4), Ga(2)–N(1) 1.9739(10), Ga(2)–C(16) 1.9902(17), N(1)–C(1) 1.3321(13), C(1)–C(2) 1.4044(13), N(1)–Ga(2)–N(1)#1 95.66(5), N(1)–Ga(2)–C(16) 115.64(4), N(1)–Ga(2)–Te(1) 112.07(3), C(16)–Ga(2)–Te(1) 105.84(5), C(1)–C(2)–C(1)#1 128.03(14), N(1)–C(1)–C(2) 123.73(11).

Open Access Article. Published on 05 February 2015. Downloaded on 12/4/2025 9:05:27 PM.
This article is licensed under a Creative Commons Attribution 3.0 Unported Licence.

Table 1 Crystallographic data of **1a**, **1b**, **2**, and **3**

	1a	**1b**	**2**	**3**
Empirical formula	$C_{58}H_{82}Ga_2N_4Te_2$	$C_{61.50}H_{86}Ga_2N_4Te_2$	$C_{41}H_{51}GaN_2Te_2$	$C_{35}H_{55}GaN_2Te$
M	1229.91	1275.98	896.75	701.13
Crystal size [mm]	0.280 × 0.220 × 0.180	0.220 × 0.180 × 0.130	0.415 × 0.326 × 0.198	0.200 × 0.190 × 0.100
T [K]	130(1)	100(1)	100(1)	100(1)
Crystal system	Monoclinic	Monoclinic	Orthorhombic	Orthorhombic
Space group	$P2_1/n$	$C2/m$	$Pbca$	$Pnma$
a [Å]	14.0688(10)	18.6322(4)	19.1512(8)	16.888(3)
b [Å]	13.8376(10)	20.9742(5)	19.7070(8)	19.798(3)
c [Å]	15.2807(11)	16.4363(4)	20.3343(8)	10.2125(15)
α [°]	90	90	90	90
β [°]	106.759(2)	98.9820(10)	90	90
γ [°]	90	90	90	90
V [Å^3]	2848.5(4)	6344.5(3)	7674.4(5)	3414.5(9)
Z	2	4	8	4
D_{calc} [g cm^{-1}]	1.434	1.336	1.552	1.364
μ (MoK$_\alpha$ [mm^{-1}])	1.988	1.788	2.237	1.668
Transmissions	0.75/0.50	0.75/0.68	0.75/0.52	0.75/0.63
F(000)	1248	2596	3568	1448
Index ranges	$-20 \le h \le 21$	$-27 \le h \le 27$	$-27 \le h \le 27$	$-25 \le h \le 23$
	$-20 \le k \le 20$	$-28 \le k \le 31$	$-27 \le k \le 26$	$-30 \le k \le 26$
	$-21 \le l \le 22$	$-24 \le l \le 24$	$-26 \le l \le 28$	$-15 \le l \le 15$
θ_{max} [°]	32.618	32.155	30.255	33.202
Reflections collected	43 835	86 728	131 905	77 225
Independent reflections	10 256	11 354	11 268	6666
R_{int}	0.0375	0.0319	0.0446	0.0307
Refined parameters	298	342	415	193
R_1 [$I > 2\sigma(I)$]^a	0.0440	0.0223	0.0469	0.0225
wR_2 [all data]^b	0.1300	0.0606	0.1249	0.0578
GooF^c	1.081	1.072	1.127	1.046
$\Delta\rho_{final}$ (max/min) [e Å^{-3}]	3.763/−1.417	0.986/−0.453	2.287/−1.586	0.677/−0.358

^{a} $R_1 = \sum(||F_o| - |F_c||)/\sum|F_o|$ (for $I > 2\sigma(I)$). ^{b} w$R_2 = \{\sum[w(F_o^2 - F_c^2)^2]/\sum[w(F_o^2)^2]\}^{1/2}$. ^{c} Goodness of fit $= \{\sum[w(|F_o^2| - |F_c^2|)^2]/(N_{observns} - N_{params})\}^{1/2}$. $w^{-1} = \sigma^2(F_o^2) + (aP)^2 + bP$ with $P = [F_o^2 + 2F_c^2]/3$, a and b are constants chosen by the program.

{[$Me_3SiNC(Ph)C(SiMe_3)_2$]Ga-μ-Te}$_2$ (2.570 Å)[27] and [i-Pr_2PNP-(i-Pr_2)TeGa-μ-Te]$_2$ (2.5783(7) Å) as well as the six-membered heterocycle [i-Pr_2PNP(i-Pr_2)TeGa-μ-Te]$_3$ (2.582(2) Å).[28] In addition, the mixed Te/carboxylate-bridged compound [R_2Ga_2(μ-Te)(μ-OOCCH$_3$)$_2$] (2.534 Å)[29] as well as the base-stabilized compounds LGa(TePh)$_3$ (L = NMe_3, PCy_3), which were obtained from the reaction of base-stabilized gallanes [$LGaH_3$] with Ph_2Te_2 and which also contain fourfold-coordinated Ga atoms and twofold-coordinated Te atoms, show comparable Ga–Te bond distances of 2.580(1) Å and 2.597(2) Å, respectively.[30] In contrast, the Ga–Te bonds in the [MeGa(TePh)$_3$]$^+$ monocation of [(Me_3P)$_4$Cu][MeGa(TePh)$_3$] is slightly elongated (2.6406(3) Å).[31] The same holds for the Ga–Te bonds in four structurally characterized Ga_4Te_4 heterocubanes, which range from 2.67 to 2.72 Å,[32–35] as well as in dimeric compounds of the general type [R_2Ga-μ-TeR]$_2$, for which Ga–Te bond lengths in the range from 2.67 to 2.76 Å were reported.[36–39] In contrast, slightly shorter Ga–Te bond lengths were reported for {[(Me_3Si)$_2$CH]$_2$Ga-μ-Te} (2.5521(4) Å),[40] [(Me_3Si)$_2$CH]$_2$GaTeSi($SiMe_3$)$_3$ (2.535(1) Å),[41] whereas the Ga–Te bonds observed in Ga{TeSi($SiMe_3$)$_3$}$_3$ (av. 2.496(6) Å)[42] as well as in Tp$^\#$GaTe (2.422(1)) (Tp$^\#$ = tris(3,5-di-*tert*-butylpyrazolyl) hydroborato), to date the only compound containing a terminal Ga–Te double bond, are significantly shortened.[43]

Reactions of trivalent group 13 compounds (MR_3, MH_3; M = Al, Ga, In) with elemental chalcogens E or chalcogen sources such as $R_3P{=}E$ (E = O, S, Se, Te) typically occur with insertion of the chalcogen atom into the M–C/H bond and subsequent formation of dimeric ([R_2M-μ-ER]$_2$) or tetrameric ([RME]$_4$) compounds, whereas divalent (R_4M_2) as well as monovalent group 13 compounds RM (M = Al, Ga, In, Tl) react with insertion of the chalcogen atom into the M–M bond.[44–49] In addition, E–Br bond cleavage reactions of PhEBr (E = Se, Te) upon treatment with the monovalent In(I) cluster [(Me_3Si)$_3$C]$_4$In$_4$[50] as well as of Te–Te bond cleavage reactions of Ph_2Te_2 by reaction with Ga(I)[26] and In(I) compounds[51] as well as with base-stabilized GaH_3[30] were reported. However, to the best of our knowledge, the cleavage of the Te–C bond of diorganyltellanes upon reaction with monovalent group 13 compounds RM has never been observed before.

Conclusions

LGa was found to selectively insert into the Te–Te bond of diphenylditellane Ph_2Te_2 as well as one Te–C bond of diisopropyltellane i-Pr_2Te, resulting in the formation of LGa(TePh)$_2$ **2** and LGa(i-Pr)Tei-Pr **3**. Moreover, its reaction with elemental tellurium yielded the Te-bridged compound [LGa-μ-Te]$_2$ **1**. We are currently investigating reactions of the somewhat stronger reducing agent LAl with various group 16 precursors. A previous report showed that LAl reacted with elemental sulfur

Open Access Article. Published on 05 February 2015. Downloaded on 12/4/2025 9:05:27 PM.
This article is licensed under a Creative Commons Attribution 3.0 Unported Licence.

with subsequent formation of $[LAl(\mu\text{-}S_3)]_2$, containing an unusual Al_2S_6 ring.[52]

Experimental

All manipulations were performed in an atmosphere of purified argon using standard Schlenk and glove-box techniques. Toluene and hexane were dried using a mBraun Solvent Purification System. THF was carefully dried over Na/K. Deuterated solvents were dried over activated molecular sieves (4 Å) and degassed prior to use. Anhydrous nature of the solvents was verified by Karl Fischer titration. The ^{1}H (300 MHz), ^{13}C{^{1}H} (75.5 MHz) and ^{125}Te NMR (95 MHz) (δ in ppm) spectra were recorded using a Bruker Avance DPX-300 spectrometer. The ^{1}H and ^{13}C{^{1}H} spectra were referenced to internal C_6D_5H (^{1}H: δ = 7.154; ^{13}C: δ = 128.39) and $C_6D_5CHD_2$ (^{1}H: δ = 2.09; ^{13}C: δ = 20.40). ^{125}Te NMR spectra were referenced to Na_2TeO_3 in D_2O. The microanalyses were performed at the elemental analysis laboratory of the University of Duisburg-Essen. IR spectra were measured with an ALPHA-T FT-IR spectrometer equipped with a single reflection ATR sampling module. Elemental tellurium and Ph_2Te_2 were commercially available and used as received, whereas i-Pr_2Te was freshly prepared according to a slightly modified procedure described for the synthesis of Te-$(SiMe_3)_2$.[53] In necessary cases, the reaction mixtures were filtered using a oven dried Teflon cannula (3.5 mm D) in which one end of the tip was wrapped with Whatman® glass microfiber filters (CAT no. 1823-025) using Teflon tape.

Synthesis of i-Pr_2Te. Et_3BHLi ("superhydride", 1.0 M in THF, 16.06 mmol, 16.1 mL) was added drop wise to a THF (50 mL) suspension of Te (1.0 g, 7.84 mmol) at 0 °C. After stirring at room temperature for 2 h, a solution of isopropyl bromide (1.976 g, 16.06 mmol, 1.5 mL) in THF (10 mL) was added. The reaction mixture was additionally stirred at room temperature for 2 h and the mixture was filtered through a glass frit. The solvents were removed under reduced pressure (500 mbar) and i-Pr_2Te was distilled at 45 °C (10 mbar). Yield: 72% (1.20 g). ^{1}H NMR (C_6D_6, 300 MHz): δ 3.18 (sept, –C*H*-$(CH_3)_2$, 2 H), 1.50 (d, –CH(C*H*$_3$)$_2$, 12 H). ^{13}C NMR (C_6D_6, 75 MHz): δ 28.00 (–*C*H$(CH_3)_2$), 10.57 (–CH(*C*H$_3$)$_2$).

Synthesis of 1. A mixture of elemental tellurium (0.0393 g, 0.308 mmol) and LGa (0.150 g, 0.308 mmol) in 20 mL of toluene was stirred at ambient temperature for 3 days. The reaction mixture was cannula filtered and the precipitate was extracted twice with 10 mL of hot toluene. Combined filtrates were concentrated to 10 mL and stored at −30 °C for 3 days to afford analytically pure **1** as pale yellow crystals. Yield: 61% (0.115 g). Anal. Calcd for $C_{58}H_{82}Ga_2N_4Te_2$·toluene: C, 59.05; H, 6.86; N, 4.24. Found: C, 59.70; H, 6.89; N, 4.26%. ^{1}H NMR (300 MHz, toluene-d_8): δ 7.10 (m, $C_6H_3(^iPr)_2$, 12 H), 4.59 (s, γ-C*H*–, 2 H), 3.33 (sept, –C*H*$(CH_3)_2$, 8 H), 1.35 (s, ArNCC*H*$_3$, 12 H), 1.10 (br m, –CH(C*H*$_3$)$_2$, 48 H). IR (neat): ν 2961 (m), 2921 (w), 2859 (w), 1530 (s), 1438 (m), 1381 (s), 1307 (s), 1257 (m), 1177 (m), 1097 (w), 1018 (m), 938 (m), 859 (m), 796 (s), 757 (m), 723 (m), 688 (w), 638 (w), 532 (w), 461 (w) cm^{-1}.

Synthesis of 2. A solution of Ph_2Te_2 (0.168 g, 0.41 mmol) in toluene (2 mL) was added dropwise to a well-stirred toluene (2 mL) solution of LGa (0.2 g, 0.41 mmol). The reaction mixture was stirred at room temperature for 3 h to give a clear yellow solution. The solution was then concentrated to 1 mL, layered with 1 mL of *n*-hexane and stored at −30 °C to give an analytically pure crystalline precipitate of **2**. Single crystals suitable for X-ray diffraction analysis were grown from *n*-hexane solution. 0.13 g of **2** was dissolved in 4 mL of warm *n*-hexane and stored at room temperature for 1 day to give yellow crystals suitable for X-ray diffraction analysis. Yield: 73% (0.269 g). Anal. Calcd for $C_{41}H_{51}GaN_2Te_2$: C, 54.91; H, 5.73; N, 3.12. Found: C, 55.30; H, 5.81; N, 3.13%. ^{1}H NMR (300 MHz, C_6D_6): δ 7.54 (m, *o-H* Ph, 4 H), 7.18 (m, $C_6H_3(^iPr)_2$, 6 H), 6.96 (m, *p-H* Ph, 2 H), 6.78 (m, *m-H* Ph, 4 H), 4.76 (s, γ-C*H*–, 1 H), 3.62 (sept, –C*H*$(CH_3)_2$, 4 H), 1.50 (s, ArNCC*H*$_3$, 6 H), 1.48 (d, –CH(C*H*$_3$)$_2$, 12 H), 1.08 (d, –CH(C*H*$_3$)$_2$, 12 H). ^{13}C NMR (75.5 MHz, C_6D_6): δ 170.63 (ArN*C*CH$_3$), 145.36 (*Ar*), 142.05 (*Ar*), 141.58 (*Ar*), 128.91 (*Ar*), 128.21 (*Ar*), 126.81 (*Ar*), 125.47 (*Ar*), 108.69 (*Ar*), 99.22 (γ-*C*H–), 29.36 (–*C*H$(CH_3)_2$), 27.01 (–CH(*C*H$_3$)$_2$), 25.44 (–CH(*C*H$_3$)$_2$), 24.67 (ArNC*C*H$_3$). ^{125}Te NMR (95 MHz, C_6D_6): δ −21.94. IR (neat): ν 3051 (w), 2962 (m), 2923 (w), 2863 (w), 1521 (m), 1460 (m), 1366 (m), 1311 (m), 1254 (m), 1169 (w), 1103 (w), 1014 (m), 935 (w), 861 (w), 797 (m), 727 (s), 689 (s), 636 (w), 531 (w), 451 (m) cm^{-1}.

Synthesis of 3. A mixture of *i*-Pr_2Te (0.068 g, 50 μL, 0.318 mmol) and LGa (0.155 g, 0.318 mmol) in 2 mL of toluene was stirred at ambient temperature for 24 h. The clear solution was concentrated to 1 mL and stored at 5 °C for 3 days to give a large amount of **2** as pale yellow blocks. Yield: 76% (0.169 g). Anal. Calcd for $C_{35}H_{55}GaN_2Te$: C, 59.96; H, 7.91; N, 4.00. Found: C, 60.10; H, 7.98; N, 3.97%. ^{1}H NMR (300 MHz, C_6D_6): δ 7.14 (m, $C_6H_3(^iPr)_2$, 6 H), 4.67 (s, γ-C*H*–, 1 H), 4.16 (sept, –C*H*$(CH_3)_2$, 2 H), 3.82 (sept, –TeC*H*$(CH_3)_2$, 1 H), 3.42 (sept, –C*H*$(CH_3)_2$, 2 H), 1.87 (d, –CH(C*H*$_3$)$_2$, 6 H), 1.61 (d, –CH(C*H*$_3$)$_2$, 6 H), 1.51 (s, ArNCC*H*$_3$, 6 H), 1.32 (m, –CH(C*H*$_3$)$_2$, 12 H), 1.08 (d, –CH(C*H*$_3$)$_2$, 6 H), 1.04 (m, –GaC*H*$(CH_3)_2$, 1 H), 0.67 (d, –GaCH(C*H*$_3$)$_2$, 6 H). ^{13}C NMR (75.5 MHz, C_6D_6): δ 169.78 (ArN*C*CH$_3$), 146.22 (*Ar*), 143.88 (*Ar*), 142.73 (*Ar*), 127.74 (*Ar*), 126.09 (*Ar*), 124.32 (*Ar*), 98.25 (γ-*C*H–), 32.51 (–*C*H$(CH_3)_2$), 29.35 (–*C*H$(CH_3)_2$), 28.48 (–*C*H$(CH_3)_2$), 25.53 (–CH(*C*H$_3$)$_2$), 25.40 (–CH(*C*H$_3$)$_2$), 24.82 (–CH(*C*H$_3$)$_2$), 24.03 (–CH(*C*H$_3$)$_2$), 21.90 (ArNC*C*H$_3$), 17.67 (–TeCH(*C*H$_3$)$_2$), 1.79 (–Ga*C*H(CH$_3$)$_2$), 1.76 (–GaCH(*C*H$_3$)$_2$). ^{125}Te NMR (95 MHz, C_6D_6): δ −115.74. IR (neat): ν 2964 (m), 2919 (w), 2849 (w), 1551 (w), 1521 (m), 1438 (m), 1383 (s), 1312 (m), 1258 (m), 1172 (w), 1098 (m), 1017 (s), 935 (w), 862 (w), 796 (s), 757 (m), 526 (m), 440 (w), 402 (w) cm^{-1}.

Single crystal X-ray diffraction

Crystallographic data of **1–3**, which were collected on a Bruker D8 Kappa APEX2 diffractometer (MoK$_\alpha$ radiation, λ = 0.71073 Å) at 130(1) K (**1a**), 100(1) K (**1b**), 100(1) K (**2**) and 100(1) K (**3**), are summarized in Table 1. The solid-state struc-

Open Access Article. Published on 05 February 2015. Downloaded on 12/4/2025 9:05:27 PM.
This article is licensed under a Creative Commons Attribution 3.0 Unported Licence.

tures of **1–3** are shown in Fig. 1–3. The structures were solved by Direct Methods (SHELXS-97) and refined anisotropically by full-matrix least-squares on F^2 (SHELXL-97).[54,55] Absorption corrections were performed semi-empirically from equivalent reflections on basis of multi-scans (Bruker AXS APEX2). The toluene molecule of **1b** is disordered *via* 2/*m* symmetry. Further solvent molecules that could not be modelled sufficiently were removed by a PLATON/SQUEEZE run.[56] The crystal quality of **2** was rather low consequently the quantitative results of the model should be carefully assessed. The resolution of the data of **3** was high enough to show a mismatch of the calculated position of H2 and the residual electron density. Consequently H2 was refined freely with its displacement parameter constrained to be 1.2 times U_{eq} of the connected C atom. Other hydrogen atoms were refined using a riding model or rigid methyl groups.

Acknowledgements

S.S. likes to thank the University of Duisburg-Essen for financial support.

Notes and references

1 N. J. Hardman, B. E. Eichler and P. P. Power, *J. Chem. Soc., Chem. Commun.*, 2000, 1991–1992.
2 N. J. Hardman and P. P. Power, *ACS Symp. Ser.*, 2002, **822**, 2–15.
3 C.-H. Chen, M.-L. Tsai and M.-D. Su, *Organometallics*, 2006, **25**, 2766–2773.
4 M. S. Hill, P. B. Hitchcock and R. Pontavornpinyo, *J. Chem. Soc., Dalton Trans.*, 2005, 273–277.
5 N. J. Hardman, P. P. Power, J. D. Gorden, C. L. B. Macdonald and A. H. Cowley, *J. Chem. Soc., Chem. Commun.*, 2001, 1866–1867.
6 C. Gemel, T. Steinke, M. Cokoja, A. Kempter and R. A. Fischer, *Eur. J. Inorg. Chem.*, 2004, 4161–4176.
7 A. Kempter, C. Gemel, T. Cadenbach and R. A. Fischer, *Organometallics*, 2007, **26**, 4257–4264.
8 A. Kempter, C. Gemel and R. A. Fischer, *Chem. – Eur. J.*, 2007, **13**, 2990–3000.
9 S. Schulz, *Chem. – Eur. J.*, 2010, **16**, 6416–6428.
10 R. J. Baker and C. Jones, *Coord. Chem. Rev.*, 2005, **249**, 1857–1869.
11 Y.-C. Tsai, *Coord. Chem. Rev.*, 2012, **256**, 722–758.
12 M. Asay, C. Jones and M. Driess, *Chem. Rev.*, 2011, **111**, 354–396.
13 G. Prabusankar, A. Kempter, C. Gemel, M.-K. Schröter and R. A. Fischer, *Angew. Chem., Int. Ed.*, 2008, **47**, 7234–7237.
14 G. Prabusankar, C. Gemel, P. Parameswaran, C. Flener, G. Frenking and R. A. Fischer, *Angew. Chem., Int. Ed.*, 2009, **48**, 5526–5529.
15 A. Seifert, D. Scheid, G. Linti and T. Zessin, *Chem. – Eur. J.*, 2009, **15**, 12114–12120.
16 N. J. Hardman and P. P. Power, *Inorg. Chem.*, 2001, **40**, 2474–2475.
17 N. J. Hardman and P. P. Power, *J. Chem. Soc., Chem. Commun.*, 2001, 1184–1185.
18 N. J. Hardman, C. Cui, H. W. Roesky, W. H. Fink and P. P. Power, *Angew. Chem., Int. Ed.*, 2001, **40**, 2172–2174.
19 C. Ganesamoorthy, D. Bläser, C. Wölper and S. Schulz, *J. Chem. Soc., Chem. Commun.*, 2014, **50**, 12382–12384.
20 C. Ganesamoorthy, D. Bläser, C. Wölper and S. Schulz, *Angew. Chem., Int. Ed.*, 2014, **53**, 11587–11591.
21 S. Gondzik, S. Schulz, D. Bläser and C. Wölper, *J. Chem. Soc., Chem. Commun.*, 2014, **50**, 1189–1191.
22 P. Steiniger, G. Bendt, D. Bläser, C. Wölper and S. Schulz, *J. Chem. Soc., Chem. Commun.*, 2014, **50**, 15461–15463.
23 S. Heimann, A. Kuczkowski, D. Bläser, C. Wölper, R. Haak, G. Jansen and S. Schulz, *Eur. J. Inorg. Chem.*, 2014, 4858–4864.
24 S. Heimann, S. Schulz, D. Bläser and C. Wölper, *Eur. J. Inorg. Chem.*, 2013, 4909–4915.
25 S. Heimann, D. Bläser, C. Wölper and S. Schulz, *Organometallics*, 2014, **33**, 2295–2300.
26 R. J. Baker, C. Jones and M. Kloth, *J. Chem. Soc., Dalton Trans.*, 2005, 2106–2110.
27 K. S. Klimek, J. Prust, H. W. Roesky, M. Noltemeyer and H.-G. Schmidt, *Organometallics*, 2001, **20**, 2047–2051.
28 M. C. Copsey and T. Chivers, *J. Chem. Soc., Chem. Commun.*, 2005, 4938–4940.
29 W. Uhl, L. Cuypers, T. Spies, F. Weller, B. Habrecht, M. Conrad, A. Greiner, M. Puchner and J. H. Wendorff, *Z. Anorg. Allg. Chem.*, 2003, **629**, 1124–1130.
30 W. J. Grigsby, C. L. Raston, V.-A. Tolhurst, B. W. Skelton and A. H. White, *J. Chem. Soc., Dalton Trans.*, 1998, 2547–2556.
31 O. Kluge and H. Krautscheid, *Inorg. Chem.*, 2012, **51**, 6655–6666.
32 S. Schulz, M. Andruh, T. Pape, T. Heinze, H. W. Roesky, L. Häming, A. Kuhn and R. Herbst-Irmer, *Organometallics*, 1994, **13**, 4004–4007.
33 C. H. Harlan, E. G. Gillan, S. G. Bott and A. R. Barron, *Organometallics*, 1996, **15**, 5479–5488.
34 U. App and K. Merzweiler, *Z. Anorg. Allg. Chem.*, 1997, **623**, 478–482.
35 W. Uhl, M. Benter, W. Saak and P. G. Jones, *Z. Anorg. Allg. Chem.*, 1998, **624**, 1622–1628.
36 M. A. Banks, O. T. Beachley Junior, H. J. Gysling and H. R. Luss, *Organometallics*, 1990, **9**, 1979–1982.
37 C. Schnitter, A. Klemp, H. W. Roesky, H.-G. Schmidt, C. Ropken, R. Herbst-Irmer and M. Noltemeyer, *Eur. J. Inorg. Chem.*, 1998, 2033–2039.
38 M. R. Kopp and B. Neumüller, *Z. Anorg. Allg. Chem.*, 1997, **623**, 796–804.
39 O. Kluge, S. Gerber and H. Krautscheid, *Z. Anorg. Allg. Chem.*, 2011, **637**, 1909–1921.

 This journal is © The Royal Society of Chemistry 2015

Open Access Article. Published on 05 February 2015. Downloaded on 12/4/2025 9:05:27 PM.
This article is licensed under a Creative Commons Attribution 3.0 Unported Licence.

40 W. Uhl and U. Schütz, *Organometallics*, 1995, **14**, 1073–1075.
41 W. Uhl, M. Layh, G. Becker, K. W. Klinkhammer and T. Hildenbrand, *Chem. Ber.*, 1992, **125**, 1547–1551.
42 S. P. Wuller, A. L. Seligson, G. P. Mitchell and J. Arnold, *Inorg. Chem.*, 1995, **34**, 4854–4861.
43 M. C. Kuchta and G. Parkin, *Inorg. Chem.*, 1997, **36**, 2492–2493.
44 C. J. Allan and C. L. B. Macdonald, in *Comprehensive Inorganic Chemistry II*, ed. J. Reedijk and K. Poeppelmeier, Elsevier, Oxford, 2013, vol. 1, pp. 485–566.
45 S. Schulz, in *Topics in Organometallic Chemistry, Vol. 41 Modern Organoaluminum Reagents*, ed. S. Woodward and S. Dagorne, Springer Verlag, 2013.
46 S. Aldridge, in *The Group 13 Metals Aluminum, Gallium, Indium and Thallium*, ed. S. Aldridge and A. J. Downs, Wiley, 2011.
47 S. Schulz, in *Comprehensive Organometallic Chemistry III*, ed. R. H. Crabtree and D. M. P. Mimgos, Compounds of Group 13–15, ed. C. E. Housecroft, Elsevier, 2007, vol. 3.
48 J. A. J. Pardoe and A. J. Downs, *Chem. Rev.*, 2007, **107**, 2–45.
49 G. He, O. Shynkaruk, M. W. Lui and E. Rivard, *Chem. Rev.*, 2014, **114**, 7815–7880.
50 W. Uhl, F. M. de Andrade, C. Peppe, J. Kösters and F. Rogel, *J. Organomet. Chem.*, 2007, **692**, 869–873.
51 C. Peppe, F. Molinos de Andrade and W. Uhl, *J. Organomet. Chem.*, 2009, **694**, 1918–1921.
52 Y. Peng, H. Fan, V. Jancik, H. W. Roesky and R. Herbst-Irmer, *Angew. Chem., Int. Ed.*, 2004, **43**, 6190–6192.
53 M. R. Detty and M. D. Seidler, *J. Org. Chem.*, 1982, **47**, 1354–1356.
54 SHELXS-97, G. M. Sheldrick, *Acta Crystallogr., Sect. A: Fundam. Crystallogr.*, 1990, **46**, 467–473.
55 G. M. Sheldrick, *SHELXL-97, Program for Crystal Structure Refinement*, Universität Göttingen, 1997 See also: G. M. Sheldrick, *Acta Crystallogr., Sect. A: Fundam. Crystallogr.*, 2008, **64**, 112–122.
56 PLATON/SQUEEZE, P. van der Sluis and A. L. Spek, *Acta Crystallogr., Sect. A: Fundam. Crystallogr.*, 1990, **46**, 194–201.